OBSERVATION OF WAKEFIELD EFFECTS WITH WIDEBAND FEEDTHROUGH-BPM AT THE POSITRON CAPTURE SECTION OF THE SuperKEKB INJECTOR LINAC

M. A. Rehman*, T. Suwada

High Energy Accelerator Research Organization (KEK), Tsukuba, Japan

Abstract

At the SuperKEKB injector linac, positrons are generated by striking electron beam at tungsten target. The secondary electrons are also produced during positron creation and accelerated in the positron capture section. A new wideband feedthrough–beam position monitor (BPM) system was developed for synchronous detection of secondary produced e^- and e^+ beams with temporal separation of about 180 ps. When e^+/e^- bunches pass through the accelerating structure or vacuum duct of different radius, they generate wakefields. These wakefields can be directly observed with the feedthrough-BPM. A simulation study has also been carried to validate the observed wakefield effects with the feedthrough-BPM. The effects of wakefields on beam parameters will be reported in this paper.

INTRODUCTION

The SuperKEKB (SKEKB) [1, 2] is an electron and positron collider with asymmetric energies to study CP violation in B mesons and also to search for new physics beyond the Standard Model, with the target luminosity of 8×10^{35} cm^{-2}s^{-1}, which is 40 time higher than its predecessor KEKB [3]. The SKEKB collider consists of e^- and e^+ rings of energy 7 GeV (HER) and 4 GeV (LER) with the stored beam current of 2.6 A and 3.6 A, respectively.

The SKEKB injector linac generates e^-/e^+ bunches of 5 nC and 4 nC to directly inject into HER and LER, respectively, at their designed energy. The low emittance e^- beam is produced by a RF–photocathode gun. The e^+ beam is produced by striking the e^- beam of energy 3.5 GeV and bunch charge of 10 nC at a tungsten target. The positrons are generated as secondary particles and have a large transverse emittance. To capture a large amount of positrons, a pulsed solenoid called flux concentrator and a large aperture S–band (LAS) accelerating structures [4] are placed in the downstream of the e^+ target. The secondary electrons are also produced in a similar amount of charges during the e^+ creation process and accelerated in the capture section. Because of phase slipping process in the capture section, the time interval between secondary produced e^- and e^+ bunches is about only 135 ps under nominal operation.

Due to low frequency response and high–frequency cable losses, conventional beam monitors, i.e., stripline beam position monitors, are difficult to detect such closely spaced and opposite polarities bunches in the capture section. For this reason in the past capture section there were no beam moni-

toring devices. As a result of a lack of information about the beam properties such as transverse positions, bunch lengths and, bunch charges, the e^+ beam suffers some amounts of beam loss after the capture section.

Therefore, a new wideband feedthrough type BPM was developed to overcome the above–mentioned challenges. This new monitor can synchronously detect e^- and e^+ bunch properties, i.e., transverse positions, bunch lengths, time interval, and bunch charges. It provides an opportunity to enhance positron beam transport through the capture section. The detailed analysis of bunch properties is reported in [5,6]. The modal analysis of electromagnetic coupling between SMA-feedthrough and beam is described in [7]. The effect of wakefields induced by the passage of e^-/e^+ bunches through the end of the accelerating structure on the BPM signal will be discussed in detail in this report.

WIDEBAND FEEDTHROUGH BEAM POSITION MONITOR

The feedthrough–BPM consists of a vacuum pipe of length 431 mm which has an inner diameter of 38 mm, four SMA-type feedthroughs having inner conductor made of Kovar with $\pi/2$ rotational symmetry are installed at the upstream direction of the vacuum pipe. The diameter of the central connector pin of feedthroughs is 1.8 mm, and they extend 1 mm to the center of the beam pipe from the inner surface of the vacuum pipe. The vacuum pipe of BPM also has bellows mounted at the downstream and upstream direction for flexible installation. The upstream bellow is shielded in order to any suppress unwanted wakefields. In the upstream direction, BPM is attached with the LAS accelerating structure. The 3-D model of the new wideband feedthrough–BPM with LAS structure is shown in Fig. 1 (a). Figure 1 (b) shows the front view of the new monitor with dimensions. Two new feedthrough–BPMs were installed in the positron capture section. The horizontal and vertical steering coils are also installed at the same locations in the capture section to optimize the e^+ transmission through the capture section. The entire capture section is enclosed in the DC solenoid coils for efficient transmission of large emittance e^+ beam. For the sake of simplicity, they have been omitted from Fig. 1. The details can be found elsewhere [2, 5].

The SMA connectors of the feedthroughs are first connected to 2 m–long semirigid coaxial cable due to its protection against a high radiation environment. Later the semirigid cable was connected to 15 m–long 10D and 2 m–long RG223 coaxial cable [8]. The RG223 coaxial cables are then connected to a real–time keysight oscilloscope of bandwidth
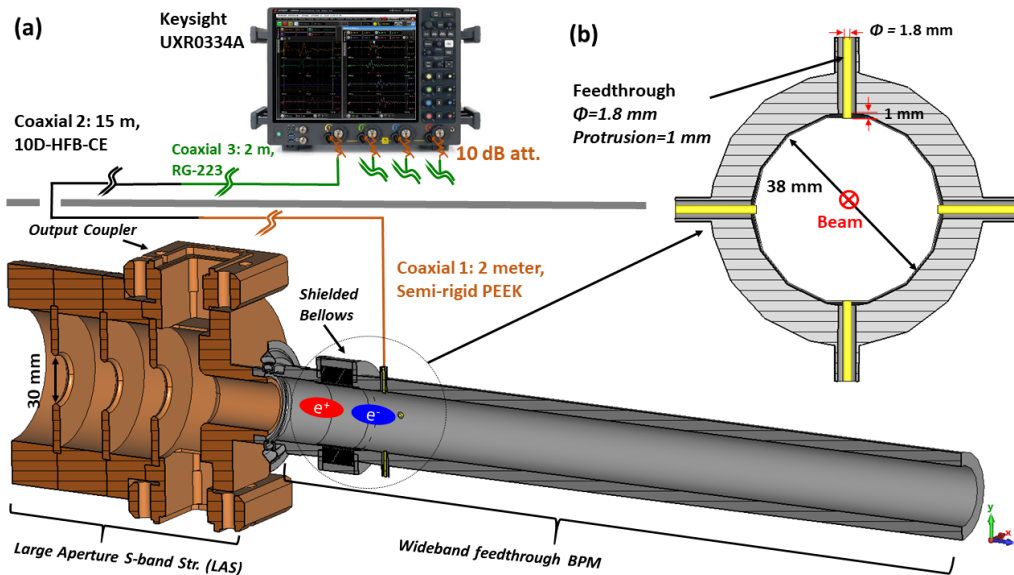
Figure 1: (a) The mechanical model of the feedthrough–BPM with LAS accelerating structure (only last three structures and output coupler). The cabling and connections of feedthrough-BPM to wideband oscilloscope are also shown. (b) Front view of the feedthrough-BPM.

33 GHz and a sampling rate of 128 GS/s [9] with a 10-dB attenuator. The cable losses have been measured in advance by a vector network analyzer [10] and are de-embedded from the feedthrough–BPM signals by the oscilloscope.

WAKEFIELD SIMULATION OF WIDEBAND FEEDTHROUGH–BPM

When a charged particle travels through any obstacle (i.e., accelerating structure, beam pipe of different radii, etc.), it generates electromagnetic (EM) fields that are left behind the particle. This EM field is called wakefield [11]. These wakefields can act on subsequent bunches (long–range wakefield) and can also act on trailing particles of the same driving bunch (short–range wakefield). In order to understand the wakefield field effect on the feedthrough-BPM signal, a time-domain simulation in CST-wakefield solver [12] has been done. In this section, simulation of single and double bunch beams and their effects for the feedthrough–BPM signals will be described.

The 3-D model used in the simulation is shown in Fig. 1 (a). Figures 2 (a) and 2 (b) present the simulation results of a single bunch e^- beam through the new monitor with and without accelerating structure, respectively. For the simulation the e^- bunch length (1σ) was assumed 10 ps with the bunch charge of 5 nC. Since the cutoff frequency in the experiment was chosen to 10 GHz by applying a 4th–order Bessel filter. Therefore, a Bessel filter with the cutoff frequency of 10 GHz is also applied to simulation results. In Fig. 2 (a) the typical bipolar signal from the feedthrough–BPM [13] (without accelerating structure) appears and after the passage of high–energy e^- bunch, a small noise appears due to the wakefield produced by the protrusion of feedthrough.
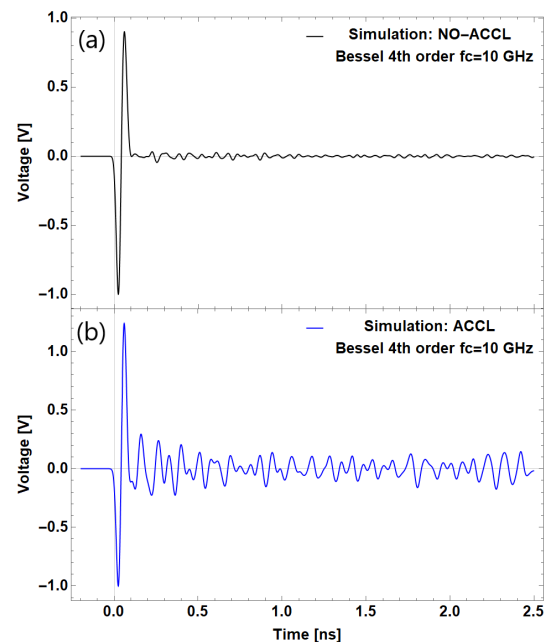

Figure 2: (a) The CST-wakefield simulation of the high–energy e^- single bunch of the feedthrough–BPM without LAS structure. No large ringing signal appears after the bipolar signal from the feedthrough–BPM. A very small noise appears only due to the 1 mm protrusion of the feedthroughs toward the center of the vacuum duct. (b) The CST-wakefield simulation of the feedthrough–BPM with the last three cavities and output coupler of LAS structure. The large ringing signal immediately appears after the bipolar signal of the e^- beam.

Whereas in the case of a simulation with the accelerating structure, a large ringing signal appears after the main bipo-
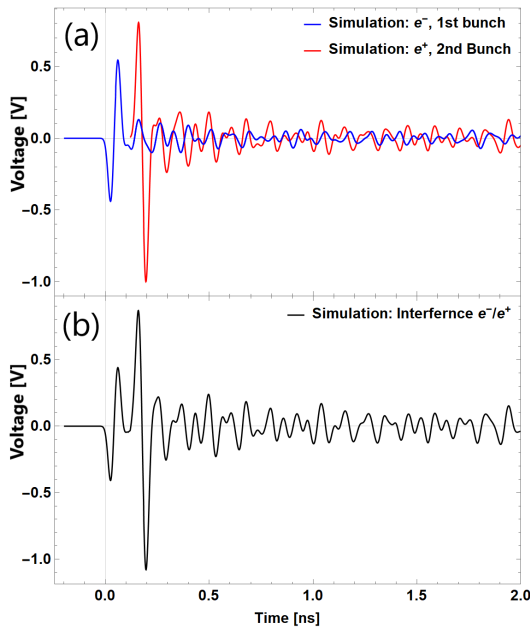
Figure 3: (a) The independent simulated signals of secondary e^- and e^+ bunches. (b) The interference of secondary e^- and e^+ signals.

lar signal as shown in Fig. 2 (b). The long–range wakefield generated by the passage of e^- bunch through the accelerating structure will reach to the feedthrough–BPM much later. Moreover, the output coupler of the accelerating structure also acts as a dumper for the higher-order modes of wakefield.

When e^- bunch passes through the end duct of accelerating structure, which has an inner diameter of 30 mm, to the feedthrough-BPM with the inner diameter of 38 mm, a wakefield produced due to this abrupt change of vacuum duct diameter. This short–range wakefield travels with the speed of light and emerges as an immediate ringing signal after the beam signal, as shown in Fig. 2 (b). Therefore, the area and bunch width for the second lobe of the bipolar signal differ with some errors from the bipolar signal without accelerating structure.

Since it is not possible to simulate the double bunch structure with the opposite polarities in the CST wakefield solver,e^- and e^+ bunches were considered independently and superimposed on each other to find the total wakefield effect. Figure 3 (a) shows the e^- and e^+ bunches independently in blue and red colors, respectively. In the nominal operation, the intensity of e^+ charges is about twice of secondary e^-, therefore e^+ intensity was assumed higher than that of the e^- bunch. The time interval between the electron and positron bunch was taken 135 ps. Figure 3 (b) shows the superposition of e^- and e^+ bunches. The e^- bunch (first bunch) exposed to only short-range wakefield, whereas the e^+ bunch experiences the wakefield generated by the e^- bunch and also self-generated wakefields. The area, bunch width, and time interval for the e^+ bunch's first lobe of the

MOPP10

54

bipolar signal differ with some errors from the bipolar signal without accelerating structure.

EXPERIMENTAL RESULTS

In order to estimate the effect of the wakefield on the experimental signal of the double bunch, it is assumed that the wakefield–induced voltage oscillates and decays [14] as follows:

$$V(t) = \sum_n a_n \sin[\omega_n t + \phi_n] e^{\frac{-\omega_n}{2Q_n}t}, \qquad (1)$$

where $V(t)$ is the induced voltage by the wakefields, n represents the mode number, ω_n resonant angular frequency of the accelerating structure, Q_n is the quality factor, and ϕ_n shows the phase delay between different excited modes.
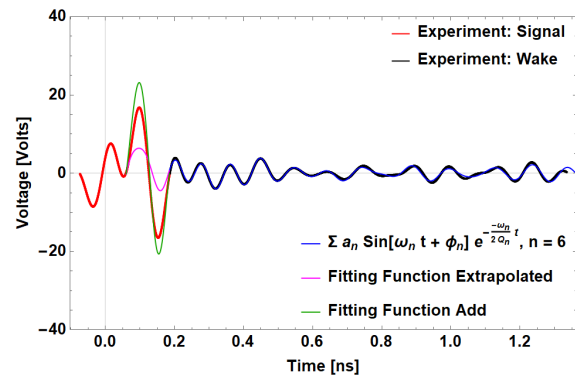

Figure 4: The synchronous signal of e^-(first)/e^+(second) bunch at nominal accelerating phase from the new feedthrough–BPM, the cutoff frequency was set to $f_c = 10\,\text{GHz}$. The fast oscillation and decay signal arises due to the wakefields of the e^-/e^+ bunches.

The model described in eq. (1) is used to fit the experimental data and then extrapolated it on the bipolar signal to estimate the effect of the wakefields on the beam parameters. Figure 4 shows the synchronous signal of e^-(first)/e^+(second) at nominal accelerating phase from the new feedthrough–BPM, the cutoff frequency was set to $f_c = 10\,\text{GHz}$. The red curve in Fig. 4 is a double bipolar signal from the e^- and e^+ bunches, whereas the curve shown in black presents induced voltage on the feedthrough–BPM due to the wakefield, which exhibits fast oscillation and decay. These wakefields induced voltages were fitted by using eq. (1) as shown in blue color in Fig. 4.

The induced voltages by the passage of the e^-/e^+ bunches through the different radius of vacuum duct are a superposition of the several higher–order modes excited by the wakefields. Therefore, fitting to experimental data was done with the different values of n. Figure 5 shows the variation in reduced χ^2 to experimental data as a function of the higher–order modes "n". It can clearly be seen at the value of $n = 6$ the reduced χ^2 value becomes ~ 1. Therefore, $n = 6$ was chosen for the fitting function.

The fitting function is also a superposition of the wakefield of e^- and e^+ bunches, as the e^- bunch is ahead of the

e^+ bunch therefore, the e^- bunch does not witness any wake-fields by the e^+ bunch. For this reason, the fitting function was extrapolated only to the bipolar signal of the e^+ bunch. In Fig. 4 the magenta curve is the extrapolation of the fitting function to the e^+ bipolar signal. The green curve in Fig. 4 shows the constructive interference of the extrapolated fitting function to the e^+ bunch. The interference of the wakefields induced voltages on the e^+ bipolar signal contributes to errors in area, bunch width, and time interval with taking into account the phase, respectively for the e^+ bunch's first lobe of the bipolar signal. The comparison of the wakefield errors for the beam parameters between experiment and simulation is summarized in Table 1. The estimated wakefield errors for the beam parameters are consistent in experiment and simulation.

Table 1: Comparison of the Wakefield Errors for Beam Parameters Between Experiment and Simulation

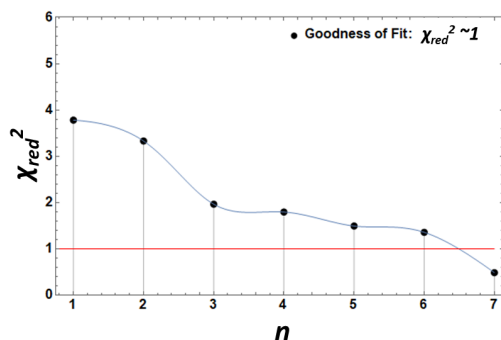| Wakefield Errors		
Beam Parameters	**Experiment**	**Simulation**
Area	41%	38%
Bunch width	1.2 ps	0.72 ps
Time Interval	2.5 ps	2.4 ps

Figure 5: Variation in the reduced χ^2 of the fitting function to the ringing signal of e^-/e^+ bunch. For $n = 6$ reduced χ^2 becomes ~ 1.

SUMMARY

The short–range wakefield has been observed as a ringing signal after a double bipolar signal in synchronous measurements of the e^- and e^+ bunches with the wideband feedthrough-BPM system at the e^+ capture section of the SuperKEKB factory. A simulation study and analytical function fitting on experimental data have been successfully carried out to estimate the effect of the wakefield on the beam parameters measured by the new beam monitor.

ACKNOWLEDGMENTS

REFERENCES

[1] K. Akai *et al.*, "SuperKEKB collider", *Nucl. Instrum. Methods Phys. Res. A*, vol. 907, p. 188, 2018. `doi:10.1016/j.nima.2018.08.017`

[2] Y. Ohnishi *et al.*, "Accelerator design at SuperKEKB", *Prog. Theor. Exp. Phys.*, vol. 2013, 03A011, 2013. `doi:10.1093/ptep/pts083`

[3] T. Abe *et al.*, "Achievements of KEKB", *Prog. Theor. Exp. Phys.*, vol. 2013, 03A001, 2013. `doi:10.1093/ptep/pts102`

[4] S. Matsumoto, T. Higo, K. Kakihara, T. Kamitani, and M. Tanaka, "Large-aperture Travelling-wave Accelerator Structure for Positron Capture of SuperKEKB Injector Linac", in *Proc. 5th Int. Particle Accelerator Conf. (IPAC'14)*, Dresden, Germany, Jun. 2014, pp. 3872–3874. `doi:10.18429/JACoW-IPAC2014-THPRI047`

[5] Tsuyoshi Suwada, Muhammad Abdul Rehman, Fusashi Miyahara, "First Simultaneous Detection of Electron and Positron Bunches at the Positron Capture Section of the SuperKEKB Factory", *Sci. Rep.* 11, 12751, 2021. `doi:10.1038/s41598-021-91707-0`

[6] M. A. Rehman, T. Suwada, and F. Miyahara, "First Synchronous Measurement of Single-Bunched Electron and Positron Beams with a Wideband Feedthrough-BPM at the Positron Capture Section of the SuperKEKB Injector Linac", presented at the 12th Int. Particle Accelerator Conf. (IPAC'21), Campinas, Brazil, May 2021, paper MOPAB163.

[7] Tsuyoshi Suwada, "Modal Analysis of Electromagnetic Couplings Between SMA-Feedthrough Electrode and Beam for Wideband Beam Monitor", presented at the 9th Int. Beam Instrumentation Conf. (IBIC'21), Pohang, Korea, Sep. 2021, paper WEPP12.

[8] Catalog of high-frequency coaxial cables, `https://www.fujikura-dia.co.jp/`.

[9] Keysight Technologies, Inc., UXR0334A Infiniium UXR-Series, `https://www.keysight.com/en/`.

[10] Keysight Technologies, Inc., N5230A PNA-L Network Analyzer, `https://www.keysight.com/en/`.

[11] M. Ferrario *et al.*, "Wakefields and Instabilities in Linear accelerators", *Proc. CAS-CERN Accel. Sch. Adv. Accel. Physics*, Trondheim, Norway, August 2013, edited by W. Herr (CERN-2014-009).

[12] CST STUDIO SUITE, `http://www.cst.com/`.

[13] R. E. Shafer, "Beam Position Monitoring", *AIP Conf. Proc.*, vol. 249, p. 601, 1992. `doi:10.1063/1.41980`

[14] A. Chao, K. H. Mess, M. Tigner and F. Zimmermann, "Handbook of Accelerator Physics and Engineering", World Scientific, 2013, pp. 264-265. `doi:10.1142/8543`